Mesenchymal Stem Cell Conditioned Medium Improves Non-alcoholic Fatty Liver Disease in Type 2 Diabetic Mice by Regulating SIRT1

Mengmeng Yang
   QILU hospital

Yixin Cui
   QILU hospital

Jia Song
   QILU hospital

Lingshu Wang
   Shandong University Qilu Hospital

Kai Liang
   QILU hospital

Sha Sha
   QILU hospital

Qin He
   QILU hospital

Chen Cui
   QILU hospital

Huiqing Hu
   Qilu Hospital

Xinghong Guo
   Qilu hospital

Nan Zang
   QILU hospital

Xiaoming Liu
   QILU hospital

Yifan Zhang
   QILU hospital

Lei Sun
   QILU Hospital

Li Chen (✉ chenli3@medmail.com.cn)
   Department of Endocrinology, Qilu Hospital of Shandong University, No. 107 Wenhua Xi Road, Jinan, 250012 Shandong China

Research

Abstract

Background

Mesenchymal stem cells (MSCs), which can be used as a cutting-edge tool in regenerative medicine, release many nutrients into their conditioned medium (CM), which has become a promising acellular treatment tool. There is increasing evidence that stem cells conditioned media can treat metabolic-related diseases (for example, Type 2 diabetes mellitus (T2DM) and diabetic endothelial dysfunction). However, their mechanism of action remains unclear. Here, we studied the potential of MSC-CM in the treatment of diabetes with non-alcoholic fatty liver disease (NAFLD) and its related molecular mechanisms.

Methods

To determine the effects of MSC-CM on NAFLD, MSC-CM was used to treat T2DM mice and palmitic acid (PA)-treated L-O2 cells. To evaluate changes in mitochondrial function and potential signaling pathways, the levels of (i) SIRT1 and PGC1α, (ii) key mitochondrial transcription factors (NRF1, TFAM, and UCP2), (iii) apoptosis-related proteins (BAX, Bcl-2, cleaved caspase-3, caspase-3, cleaved PARP, and PARP), and (iv) inflammation-related proteins (TNF-α, IL-1β, and IL-6) were assessed by western blotting.

Results

MSC-CM improves insulin resistance in diabetic mice, corrects the pathological structure of the liver, enhances the liver's total antioxidant capacity and mitochondrial function (both in vivo and in vitro), reduces inflammation, and reduces cell apoptosis. In addition, SIRT1 expression may contribute to the effect of MSC-CM treatment. We found that MSC-CM enhanced the expression of SIRT1 and downstream target proteins in the liver of T2DM mice and L-O2 cells treated with PA. At the same time, transfection of SIRT1 siRNA weakened the therapeutic effects of MSC-CM on the liver.

Conclusions

Our findings indicate that MSC-CM improves NAFLD in T2DM mice by regulating the expression level of SIRT1, which provides new evidence that MSC-CM has the potential to treat T2DM patients with NAFLD clinically.

Introduction

Non-alcoholic fatty liver disease (NAFLD) is a series of liver diseases, defined by the presence of steatosis in more than 5% of liver cells with little or no alcohol consumption [1]. NAFLD includes the benign non-alcoholic fatty liver (NAFL) and the more serious non-alcoholic steatohepatitis (NASH). Obesity, insulin resistance, and diabetes are closely related to the accumulation of excessive lipids in the liver parenchyma. NAFLD is characterized by excessive accumulation of lipids in liver cells and is the most common chronic liver disease in the world. In the past few decades, the prevalence of NAFLD has risen sharply. Studies have shown that up to 70% of diabetic patients suffer from NAFLD [2, 3]. There is a

strong association between NAFLD and diabetes risk [4, 5]. When a patient is diagnosed with NAFLD, the risk of developing diabetes increases by approximately five times [6]. Diabetes can also increase the risk of NAFLD progression [7-9]. Among 432 patients with NAFLD confirmed by biopsy, coexisting type 2 diabetes (T2DM) was found to be an independent risk factor for liver fibrosis [10]. Compared with any condition that exists alone, coexisting NAFLD is associated with serious adverse consequences of diabetes.

In the past 10 years, mesenchymal stem cells (MSCs) have become the most promising resource for cell transplantation due to their immunoregulatory function [11], paracrine function [12], and trans-differentiation regulatory function [13]. Extensive studies have shown that human umbilical cord mesenchymal stem cells (Hu-MSCs) reduce liver fibrosis in rats [14] and improve NAFLD in obese mice [15], highlighting their ability to reduce liver cell damage. However, the known treatments of MSCs have their own limitations, including residency in organs [16], a lack of effective utilization [17], a low survival rate in vivo [18], and the potential for tumorigenicity of implanted MSCs [19], which may hinder the development of stem cell therapy. However, the cell-free MSC conditioned medium (CM) is rich in nutrients, such as growth factors and cytokines, and is easily available, making the application of MSC-CM an alternative treatment option. Related studies based on MSC-CM have shown that MSC-CM can improve diabetic endothelial dysfunction [20] and reduce renal fibrosis [21]. However, the potential protective effects of MSC-CM on NAFLD in diabetes and the exact mechanism of action are still unclear.

Mitochondria are organelles with a double-membrane structure. They are the energy generators of cells and play a central role in the oxidation of nutrients to produce energy [22]. A large number of studies have shown that mitochondrial dysfunction plays an important role in the occurrence and progression of NAFLD [22, 23]. Mitochondrial dysfunction (especially oxidative respiratory chain defects) plays a key role in the physiopathology of NASH. Oxidative stress is the key to the pathogenesis of NAFLD, and its main feature is the production of reactive oxygen species (ROS). In NAFLD, mitochondrial dysfunction is the main cause of ROS accumulation. Dysfunction of the oxidative respiratory chain and impaired lipid peroxidation (caused by mitochondrial dysfunction) further increase the production of ROS. The production of ROS will in turn aggravate lipid peroxidation and cause a variety of harmful effects to liver cells and other cells. The production of highly reactive aldehyde derivatives (such as malondialdehyde), further forming a vicious circle, may damage mitochondrial proteins and mitochondrial DNA (mtDNA) [9, 24], further suggesting that mitochondrial dysfunction will aggravate the severity of NAFLD [25]. Therefore, improving mitochondrial function is a potential treatment strategy for reducing NAFLD [26].

Sirtuin 1 (SIRT1) is the first member of the mammalian homologues of the class III histone deacetylases. SIRT1 regulates lifespan and cell metabolism. SIRT1 can mediate the deacetylation of downstream target proteins such as peroxisome proliferator-activated receptor gamma coactivator 1α (PGC1α) to participate in fatty acid oxidation and mitochondrial biogenesis and function [27-29]. Upregulation of SIRT1 effectively reduces obesity and insulin resistance in NAFLD rodents [30], whereas downregulation or complete silencing of SIRT1 can exacerbate fatty liver and inflammation [31]. In obesity and NAFLD patients, the expression of SIRT1 was found to be reduced in plasma and the liver [32, 33].

The purpose of the present study was to use in vitro palmitic acid (PA)-treated human primary hepatocytes (L-O2 cells) and a streptozotocin (STZ)-treated diabetic mouse model to explore the potential therapeutic effects of MSC-CM on diabetes with NAFLD. We further explored whether the observed effects depend on the improvement of mitochondrial function. We found that the SIRT1 signal transduction pathway plays an important role in the underlying molecular mechanisms. These findings shed new light on the potential of cell-free CM to treat diabetes mellitus combined with NAFLD.

Materials And Methods

Cell culture and treatment

With the approval of the ethics committee of Qilu Hospital of Shandong University, we obtained full-term human umbilical cords through cesarean section. All participants signed an informed consent form for the use of umbilical cord in this study. After washing the umbilical cord three times in saline, the arteries and veins were removed, and then the interstitial tissue of Wharton's jelly was exposed. Then, the tissue was cut into small pieces with sterile scissors and placed in a cell culture flask containing 20% fetal bovine serum (FBS) in α-MEM (Gibco, MD, USA), which was placed in an incubator at 37°C containing 5% CO_2. We changed the medium every three days. The third to seventh passages of cells were used for experiments.

Human L-O2 cells were purchased from the China Cell Culture Center (Shanghai, China) and stored in DMEM (Hyclone, UT, USA) with 10% FBS and placed at 37°C with 5% CO_2. L-O2 cells were incubated with 0.4 mM PA (Sigma-Aldrich, USA) for 48 h to establish an NAFL cell model or with PA and MSC-CM. To further evaluate the effects of MSC-CM on PA-treated hepatocytes, SIRT1 was knocked down using specific small interfering RNA (siRNA) (GenePharma, China) and Lipofectamine™ 2000 transfection reagent (ThermoFisher, USA) according to the manufacturer's instructions.

Animal experiments

A total of 45 male 6-week-old C57BL/6 mice (about 20 g each) were purchased from Synergy Pharmaceutical Bioengineering Co., Ltd. (Nanjing, China). After 2 weeks of adaptive feeding, the mice were randomly divided into the following two groups: normal chow diet (NCD, n = 15) and 45% high fat diet (HFD, n = 30). After 8 weeks of feeding the HFD and 12 h of fasting, these mice were injected with STZ (100 mg/kg, S0130; Sigma-Aldrich) intraperitoneally. If two consecutive fasting blood glucose levels were ≥16.7 mM, the T2DM model was considered successfully established. The T2DM mice were divided into two groups (n = 15 per group): the control (PBS) group and the MSC-CM group. Then, as mentioned above, after STZ injection, 200 μl PBS and MSC-CM were injected weekly through the tail vein, once every three days, for three consecutive months.

Preparation of MSC-CM from human umbilical cord mesenchymal stem cells (Hu-MSCs)

Hu-MSCs were inoculated into culture flasks. When the MSCs were fused, the medium was changed to serum-free medium and cells were cultured for an additional 24 h. Then the supernatant was collected, and a centrifugal filter device (Ultracel-10K; Millipore, Billerica, MA) was used with a cut-off value of 10 kDa to perform ultrafiltration on the MSC supernatant according to the manufacturer's instructions to produce MSC-CM (final concentration: 1 mg/mL), which was filtered with a 0.2 µm filter and stored at −80°C until use.

Metabolic parameter analysis

Body weight and fasting blood glucose were monitored weekly. Serum alanine aminotransferase (ALT), aspartate aminotransferase (AST), triglyceride (TG) and total cholesterol (TC) were detected using ELISA kits (ColorfulGene Biological Technology, Wuhan, China). After fasting for 12–16 h, the intraperitoneal glucose tolerance test (IPGTT) was performed by injecting glucose (2 g/kg, Sigma-Aldrich). After fasting for 6 h, the intraperitoneal insulin resistance test (IPITT) was performed by injecting insulin (0.75 IU/kg, Jiangsu Wanbang Pharmaceutical, China). Then blood was collected from the tip of the tail vein at 0, 30, 60, 90, 120, and 180 min for glucose measurement. Before the anesthetized mice were euthanized, the body fat mass of the mice was measured by a dual-energy X-ray absorption method (DEXA, Ge Lunar Prodigy, USA) (n = 7 per group). Then, the liver tissue was harvested and stored in liquid nitrogen or fixed with 4% phosphate buffered formaldehyde (PBF).

Western blot analysis

The cells were harvested and lysed in RIPA buffer. The protein concentration was measured with a BCA analysis kit (P0012S, Beyotime, Shanghai, China). After SDS-PAGE and transfer to a membrane, the membrane was incubated with the primary antibody overnight at 4°C and then with the horseradish peroxidase-labeled secondary antibody. Protein bands were imaged using Image Lab software (BioRad, USA). The intensity of protein bands was measured by ImageJ and normalized to β-actin.

The primary antibodies were as follows: SIRT1 (CST, USA, Cat: 9475), PGC1α(Proteintech

, China, Cat: 20658-1-AP), NRF1(Proteintech, China, Cat: 124821-1-AP), TFAM (Proteintech, China, Cat: 22586-1-AP), UCP2 (Proteintech, China, Cat: 11081-1-AP), TNF-α (BIOSS, China, Cat: bs-2081R), IL-1β (BIOSS,China,Cat:bs-6319R), IL-6 (Proteintech, China, Cat: 66146-1-Ig), Bax (CST, USA, Cat: 2772), Bcl-2 (ImmunoWay, USA, Cat: YM3041), cleaved caspase-3 (CST, USA, Cat: 9664), caspase-3(CST, USA, Cat: 9662), cleaved-PARP (CST, USA, Cat: 5625), PARP (CST, USA, Cat: 9542),β-actin (CST, USA, Cat: 4970).

Small interfering RNA transfection

For RNA silencing, GenePharma designed and synthesized an siRNA sequence targeting human *SIRT1*. The *SIRT1* siRNA sequence was 5'-CCA AGC AGC UAA GAG UAA UTT-3'. The negative control (NC) siRNA targeted the following sequence: 5'-UUC UCC GAA CGU GUC ACG UTT-3'. L-O2 cells were transfected with 160 pmol siRNA with Lipofectamine 2000 transfection reagent (Invitrogen, USA) for 6–8 h according to the manufacturer's instructions.

Hematoxylin and eosin (HE) staining

The liver tissue slices were processed according to standard hematoxylin and eosin (HE) staining techniques, and then the pathological changes of these tissues were observed under an optical microscope. The paraffin sections were deparaffinized and washed in PBS, and then incubated in preheated 10 mM sodium citrate buffer at 95°C for 15 min. The slides were washed, incubated with 3,3'-diaminobenzidine (DAB) as a chromogen, and then examined under an optical microscope.

Glycogen periodic acid Schiff staining

For periodic acid Schiff (PAS) staining, the liver sections were washed three times with PBS for 5 min each time and then incubated with periodic acid for 8 min. After washing twice in distilled water, the sections and cells were stained with Schiff reagent for 20 min, rinsed with distilled water three times, stained with hematoxylin, and then examined under a microscope.

Oil Red O staining

The frozen sections were stained with Oil Red O using the Oil Red O Staining Kit (#D027; Jiancheng Biotechnology Co., Ltd., China) according to the manufacturer's instructions.

Terminal deoxynucleotidyl transferase dUTP nick-end labeling staining

After washing with PBS, the L-O2 cell slides were fixed in 4% paraformaldehyde (P1110; Solarbio) for 1 h and then permeabilized with 0.5% Triton X-100 for 10 min. A terminal deoxynucleotidyl transferase dUTP nick-end labeling (TUNEL) assay was performed using the in situ cell death detection kit, POD (11684817910; Roche, USA). After deparaffinization of the liver paraffin section with xylene, the in situ cell death detection kit and TMR red (12156792910; Roche) were used to perform TUNEL staining according to standard methods.

Detection of intracellular ROS

The dichlorodihydrofluorescein diacetate Reactive Oxygen Species Determination Kit (Beyotime, China) was used according to the manufacturer's instructions to measure intracellular ROS levels.

Total antioxidant capacity test

The 2,2'-azino-bis-3-ethylbenzothiazoline-6-sulfonic acid Assay Kit (Beyotime, China) was used according to the manufacturer's instructions to test the total antioxidant capacity.

Statistical analysis

All experiments were repeated at least three times. The results are reported as the mean ± standard error of the mean (SEM). The statistical differences between the groups were determined by the paired Student

t-test or by one-way analysis of variance (ANOVA) using GraphPad Prism 8 software (San Diego, California, USA). *P* < 0.05 was considered to indicate statistical significance.

Results

MSC-CM improves glucose tolerance in T2DM mice and increases insulin sensitivity

To determine whether MSC-CM has therapeutic effects in T2DM mice, Hu-MSCs were first isolated and identified. To identify Hu-MSCs, the surface marker levels and the multi-lineage differentiation ability of adherent cells were first examined. The results of Oil Red O staining and Alizarin Red staining indicate that Hu-MSCs have the potential to differentiate into adipocytes(Fig.1a) and osteoblasts(Fig.1b). Then, flow cytometry analysis was used to characterize Hu-MSCs by determining whether they express surface markers such as CD105 and CD73. These markers were enriched in Hu-MSCs, while the negative markers HLA-DR and CD34 exhibited low expression(Fig.1c).

Next, we established a T2DM mouse model by feeding HFD and injecting the mice with STZ. MSC-CM was injected into mice through the tail vein, and PBS (200 μl) was used as a negative control. As shown in the figure, MSC-CM significantly reduced the body weight and body fat percent of T2DM mice(Fig.1d,e). The IPGTT and IPITT results revealed that MSC-CM significantly improved glucose metabolism and insulin sensitivity in T2DM mice. These data indicate that MSC-CM improves glucose tolerance and insulin sensitivity in T2DM mice(Fig.1f,g).

MSC-CM ameliorated the pathological changes and blood lipids in the livers of T2DM mice and alleviated liver dysfunction

We further observed the effects of MSC-CM on the liver structure of T2DM mice. HE staining showed that the liver structure of the T2DM group was disordered, and steatosis and vacuolar changes were increased, while in the livers of T2DM mice treated with MSC-CM, tissue structure improved, and steatosis and vacuolar changes were reduced. Glycogen staining revealed that glycogen deposition in the T2DM group was reduced, and glycogen accumulation was higher in the MSC-CM intervention group compared with the PBS group. Oil Red O staining revealed that lipid droplets in the T2DM group were significantly increased, and lipid droplets in the MSC-CM group were significantly reduced compared with the PBS group(Fig.2a). Then, we analyzed the effects of MSC-CM on liver dysfunction and the blood lipid profile. Compared with the control group, the liver ALT(Fig.2b) and AST(Fig.2c) levels and the blood TC(Fig.2d) and TG(Fig.2e) levels were significantly increased in T2DM mice, while in T2DM mice treated with MSC-CM they were significantly lower compared with the PBS treatment group, indicating that MSC-CM alleviated liver dysfunction of T2DM mice and improved the lipid distribution.

MSC-CM enhances liver mitochondrial function and reduces inflammation and apoptosis

Mitochondrial function plays a key role in maintaining normal energy metabolism, and mitochondrial dysfunction is one of the main causes of NAFLD. SIRT1 mediates the deacetylation of PGC1α. The

downstream transcription factors NRF1(nuclear respiratory factor 1), TFAM(mitochondrial transcription factor A), and UCP2(uncoupling protein 2) of PGC1α are all key to maintaining mitochondrial function. We found that the protein levels of SIRT1, PGC1α, NRF1, TFAM, and UCP2 in the liver cells of T2DM mice were lower compared with the normal control group, while the protein levels increased after MSC-CM treatment(Fig.3a,b). Compared with normal mice, the levels of pro-inflammatory cytokines TNF-α, IL-1β, and IL-6 in the livers of diabetic mice were significantly increased, while the expression levels of pro-inflammatory cytokines decreased after MSC-CM intervention(Fig.3c). Further evaluating the degree of liver cell damage, it was found that the ratio of BAX (a pro-apoptotic protein) to Bcl-2 (an anti-apoptotic protein) in liver cells of T2DM mice increased, and the protein levels of apoptotic markers (cleaved caspase-3/caspase-3 and cleaved PARP/PARP) were significantly increased, and the ratios of BAX/Bcl-2, cleaved PARP/PARP, and cleaved caspase-3/caspase-3 were lower after MSC-CM intervention than in the PBS group(Fig.3d). TUNEL staining indicated that the proportion of TUNEL-positive (apoptotic) cells in T2DM livers was significantly increased, and the proportion of TUNEL-positive (apoptotic) cells was reduced after MSC-CM treatment compared with the PBS group(Fig.3f). The total oxidative capacity of liver cells was measured using a commercial kit, and the results showed that the Trolox equivalent antioxidant capacity (TEAC) of T2DM liver cells decreased, while the total antioxidant capacity of the cells increased after MSC-CM intervention(Fig.3e).

The effects of MSC-CM on L-O2 cells treated with PA in vitro

In order to verify the specific mechanism by which MSC-CM protects liver cells, PA and PA+MSC-CM were used to stimulate L-O2 cells. We found that the in vitro results were consistent with the in vivo experimental findings: SIRT1 and PGC1α were down-regulated in L-O2 cells stimulated by PA(Fig.4a). The expression of downstream transcription factors NRF1, TFAM, and UCP2 decreased(Fig.4b). While, the expressions of SIRT1 and PGC1α in L-O2 cells treated with MSC-CM were higher than those in the PA treatment group(Fig.4a), the expressions of the downstream transcription factors NRF1, TFAM and UCP2 were also higher than those in the PA treatment group(Fig.4b). The PA-treated L-O2 cells pro-inflammatory cytokine TNF-α, IL-1β, and IL-6 are up-regulated, but down-regulated in the MSC-CM treatment group(Fig.4c). Apoptosis indicators BAX/Bcl-2, cleaved caspase 3/caspase 3 and cleaved PARP/PARP are increased in PA-treated L-O2 cells, while the expression was decreased after MSC-CM treatment(Fig.4d). TUNEL staining also proved that MSC-CM reduced the apoptosis of L-O2 cells treated with PA(Fig.4f). Finally, we tested the total antioxidant capacity and ROS production of the cells. The results showed that MSC-CM enhanced the total antioxidant capacity of the cells after PA treatment(Fig.4e) and reduced the production of ROS(Fig.5a). Overall, these data indicate that MSC-CM has positive therapeutic effects on L-O2 cells in vitro.

MSC-CM maintains the biological functions of mitochondria through the SIRT1 pathway, and after SIRT1 is silenced, the antioxidant, anti-inflammatory, and apoptotic effects of MSC-CM are offset

To verify whether SIRT1 is essential for maintaining mitochondrial function, siRNA was used to silence SIRT1 expression to observe changes in L-O2 cell mitochondrial function. The results showed that after

silencing SIRT1, the effects of MSC-CM on the SIRT1, PGC1α, NRF1, TFAM, and UCP2 proteins levels in L-O2 cells were significantly offset(Fig.5b,c), ROS production increased(Fig.6c), and the total antioxidant capacity decreased(Fig.6b). After SIRT1 siRNA was transfected into L-O2 cells, MSC-CM could not reduce the BAX/Bcl-2, cleaved PARP/PARP, and cleaved caspase 3/caspase 3 ratios(Fig.5e), TUNEL staining showed increased apoptosis(Fig.6a),, and the levels of the pro-inflammatory cytokines TNF-α, IL-1β, and IL-6 increased(Fig.5d),, confirming that SIRT1 mediates the protective effects of MSC-CM on liver cells.

Discussion

Globally, the incidence of NAFLD is increasing [34]. It is estimated that the global prevalence of NAFLD is as high as 1 billion [35]. NAFLD is caused by excessive lipid accumulation in the liver, and the presence of NAFLD is an indicator of insulin resistance [36]. Therefore, NAFLD is generally regarded as a liver manifestation of metabolic syndrome. In addition, it is a major risk factor for T2DM and is usually found as a comorbidity in patients with T2DM [37].

The molecular mechanisms underlying the development from steatosis and steatohepatitis to advanced liver disease and from steatosis to severe liver damage are not fully understood. Complex processes in the mitochondria play a central role, including energy and ROS production, calcium homeostasis, the regulation of apoptosis, and lipid metabolism [38]. Recent studies have shown that ROS are overproduced, thereby exacerbating mitochondrial dysfunction and increasing the vicious circle of liver cell oxidative damage being involved in the occurrence and progression of NAFLD [39]. In NAFLD, oxidative stress and lipid peroxidation induce the production of pro-inflammatory cytokines, including TNF-α, IL-1β, and IL-6 [40]. Excessive production of ROS and reduced antioxidant defenses can also damage mtDNA. Oxidative damage to nuclear DNA may amplify mitochondrial damage by endangering the transcription of key mitochondrial proteins. It has been reported that the expression levels of PGC1α, TFAM, and NRF1, the key regulatory factors involved in mitochondrial metabolism and organelle biogenesis in NAFLD, are reduced [41, 42]. Their upstream target protein SIRT1 has been identified as a potential therapeutic target for NAFLD [43].

Recent research has indicated that MSC-CM therapy has several big advantages compared with MSC transplantation therapy. MSC-CM is rich in nutrients, is easy to obtain, has a high utilization rate, and does not increase potential tumorigenicity. Studies have shown that MSC-CM has positive effects in disease treatment, further highlighting the broad prospects of MSC-CM in the application of liver diseases.

Our research has shed light on the great potential of MSC-CM in the treatment of diabetes and NAFLD. MSC-CM can not only improve insulin resistance and increase insulin sensitivity in T2DM mice, but also relieve liver dysfunction and improve the blood lipid profile. It is further found that MSC-CM can reduce inflammation and apoptosis and enhance the antioxidant capacity by maintaining mitochondrial function, thereby reducing the damage of NAFLD liver cells associated with diabetes. In vitro, MSC-CM had the same effect on PA-treated L-O2 hepatocytes. MSC-CM increased the expression of SIRT1, PGC1α,

NRF1, TFAM, and UCP2 in PA-treated L-O2 cells, enhanced the total antioxidant capacity of the cells, improved the expression levels of pro-inflammatory cytokines, and reduced apoptosis. After silencing SIRT1, the positive effects of MSC-CM were partially offset. We conclude that MSC-CM can improve NAFLD in diabetic mice by regulating the expression of SIRT1.

Recent studies provided more insights into the role of SIRT1 in maintaining normal liver development and function [44] and the effects of SIRT1 activators on fatty liver disease [45, 46]. SIRT1 enhances the antioxidant capacity by deacetylating FOXO and PGC1α, thereby protecting the liver against oxidative stress, and reducing local and circulatory conditions by deacetylating NF-κB in hepatic and adipose tissue. In our study, we explored the relationship between MSC-CM, NAFLD, and SIRT1, and found that MSC-CM can act as an agonist of SIRT1, significantly upregulate the expression level of SIRT1 in liver cells, and improve NAFLD. In summary, our findings elucidate a new molecular mechanism underlying the effects of MSC-CM, which can prevent and/or treat diabetes and its related fatty liver disease.

Conclusions

In summary, our current results indicate that MSC-CM can effectively alleviate NAFLD by enhancing the biological functions of mitochondria, reducing inflammation, and inhibiting cell apoptosis in T2DM models both in vivo and in vitro and that these efficacies were associated with the upregulation of SIRT1. Taken together, our findings clarify a new molecular mechanism related to MSC-CM-based therapies that can prevent and/or treat diabetes and its related liver disease.

Abbreviations

MSCs Mesenchymal stem cells

Hu-MSCs Human umbilical cord mesenchymal stem cells

MSC-CM Mesenchymal stem cell-conditioned medium

T2DM Type 2 diabetes mellitus

NAFLD Non-alcoholic fatty liver disease

IPGTT Intraperitoneal glucose tolerance test

IPITT Intraperitoneal insulin tolerance test

AUC Area under the curve

FBS Fetal bovine serum

PBS Phosphate-buffered saline

HFD High-fat diet

NCD Normal chow diet

CON Control

ALT Alanine aminotransferase

AST Aspartate aminotransferase

TC Total cholesterol

TG Triglyceride

ROS Reactive oxygen species

Declarations

Availability of data and materials

The datasets used and analyzed during the current study are available from the corresponding authors on reasonable request.

Ethics approval and consent to participate

With the approval of the Ethics Committee at Qilu Hospital of Shandong University, all participants provided informed consent for the use of the umbilical cord in this experimental study. All animal experiments were conducted in accordance with the Animal Ethics Committee of Shandong University.

Consent for publication

Not applicable.

Competing interests

The authors declare that they have no competing interests.

Footnotes

Publisher's Note

Springer Nature remains neutral with regard to jurisdictional claims in published maps and institutional affiliations.

Contributor Information

Lei Sun, Email:13969193236@163.com.

Li Chen, Email: chenli3@medmail.com.cn.

References

1. Cobbina, E. and F. Akhlaghi, *Non-alcoholic fatty liver disease (NAFLD) - pathogenesis, classification, and effect on drug metabolizing enzymes and transporters.* Drug Metab Rev, 2017. **49**(2): p. 197-211.
2. Williamson, R.M., et al., *Prevalence of and risk factors for hepatic steatosis and nonalcoholic Fatty liver disease in people with type 2 diabetes: the Edinburgh Type 2 Diabetes Study.* Diabetes Care, 2011. **34**(5): p. 1139-44.
3. Targher, G., et al., *Prevalence of nonalcoholic fatty liver disease and its association with cardiovascular disease among type 2 diabetic patients.* Diabetes Care, 2007. **30**(5): p. 1212-8.
4. Loria, P., A. Lonardo, and F. Anania, *Liver and diabetes. A vicious circle.* Hepatol Res, 2013. **43**(1): p. 51-64.
5. Takamura, T., et al., *Fatty liver as a consequence and cause of insulin resistance: lessons from type 2 diabetic liver.* Endocr J, 2012. **59**(9): p. 745-63.
6. Hillenbrand, A., et al., *Prevalence of non-alcoholic fatty liver disease in four different weight related patient groups: association with small bowel length and risk factors.* BMC Res Notes, 2015. **8**: p. 290.
7. Bril, F. and K. Cusi, *Management of Nonalcoholic Fatty Liver Disease in Patients With Type 2 Diabetes: A Call to Action.* Diabetes Care, 2017. **40**(3): p. 419-430.

8. Younossi, Z.M., et al., *Nonalcoholic fatty liver disease in patients with type 2 diabetes.* Clin Gastroenterol Hepatol, 2004. **2**(3): p. 262-5.

9. Paradies, G., et al., *Oxidative stress, cardiolipin and mitochondrial dysfunction in nonalcoholic fatty liver disease.* World J Gastroenterol, 2014. **20**(39): p. 14205-18.

10. Hossain, N., et al., *Independent predictors of fibrosis in patients with nonalcoholic fatty liver disease.* Clin Gastroenterol Hepatol, 2009. **7**(11): p. 1224-9, 1229.e1-2.

11. Castro-Manrreza, M.E. and J.J. Montesinos, *Immunoregulation by mesenchymal stem cells: biological aspects and clinical applications.* J Immunol Res, 2015. **2015**: p. 394917.

12. Yu, B., X. Zhang, and X. Li, *Exosomes derived from mesenchymal stem cells.* Int J Mol Sci, 2014. **15**(3): p. 4142-57.

13. Rosset, P., F. Deschaseaux, and P. Layrolle, *Cell therapy for bone repair.* Orthop Traumatol Surg Res, 2014. **100**(1 Suppl): p. S107-12.

14. Chai, N.L., et al., *Umbilical cord-derived mesenchymal stem cells alleviate liver fibrosis in rats.* World J Gastroenterol, 2016. **22**(26): p. 6036-48.

15. Li, B., et al., *Human Umbilical Cord-Derived Mesenchymal Stem Cell Therapy Ameliorates Nonalcoholic Fatty Liver Disease in Obese Type 2 Diabetic Mice.* Stem Cells Int, 2019. **2019**: p. 8628027.

16. Nagaishi, K., et al., *Mesenchymal stem cell therapy ameliorates diabetic hepatocyte damage in mice by inhibiting infiltration of bone marrow-derived cells.* Hepatology, 2014. **59**(5): p. 1816-29.

17. Osugi, M., et al., *Conditioned media from mesenchymal stem cells enhanced bone regeneration in rat calvarial bone defects.* Tissue Eng Part A, 2012. **18**(13-14): p. 1479-89.

18. Zimmermann, C.E., et al., *Survival of transplanted rat bone marrow-derived osteogenic stem cells in vivo.* Tissue Eng Part A, 2011. **17**(7-8): p. 1147-56.

19. Barkholt, L., et al., *Risk of tumorigenicity in mesenchymal stromal cell-based therapies--bridging scientific observations and regulatory viewpoints.* Cytotherapy, 2013. **15**(7): p. 753-9.

20. Yuan, Y., et al., *Mesenchymal stem cell-conditioned media ameliorate diabetic endothelial dysfunction by improving mitochondrial bioenergetics via the Sirt1/AMPK/PGC-1α pathway.* Clin Sci (Lond), 2016. **130**(23): p. 2181-2198.

21. Liu, B., et al., *Human umbilical cord mesenchymal stem cell conditioned medium attenuates renal fibrosis by reducing inflammation and epithelial-to-mesenchymal transition via the TLR4/NF-κB signaling pathway in vivo and in vitro.* Stem Cell Res Ther, 2018. **9**(1): p. 7.

22. Nassir, F. and J.A. Ibdah, *Role of mitochondria in nonalcoholic fatty liver disease.* Int J Mol Sci, 2014. **15**(5): p. 8713-42.

23. Begriche, K., et al., *Mitochondrial adaptations and dysfunctions in nonalcoholic fatty liver disease.* Hepatology, 2013. **58**(4): p. 1497-507.

24. Begriche, K., et al., *Mitochondrial dysfunction in NASH: causes, consequences and possible means to prevent it.* Mitochondrion, 2006. **6**(1): p. 1-28.

25. Petrosillo, G., et al., *Mitochondrial dysfunction in rat with nonalcoholic fatty liver Involvement of complex I, reactive oxygen species and cardiolipin.* Biochim Biophys Acta, 2007. **1767**(10): p. 1260-7.

26. Perry, R.J., et al., *Controlled-release mitochondrial protonophore reverses diabetes and steatohepatitis in rats.* Science, 2015. **347**(6227): p. 1253-6.

27. Tang, B.L., *Sirt1 and the Mitochondria.* Mol Cells, 2016. **39**(2): p. 87-95.

28. Rodgers, J.T. and P. Puigserver, *Fasting-dependent glucose and lipid metabolic response through hepatic sirtuin 1.* Proc Natl Acad Sci U S A, 2007. **104**(31): p. 12861-6.

29. Sathyanarayan, A., M.T. Mashek, and D.G. Mashek, *ATGL Promotes Autophagy/Lipophagy via SIRT1 to Control Hepatic Lipid Droplet Catabolism.* Cell Rep, 2017. **19**(1): p. 1-9.

30. Li, Y., et al., *Hepatic overexpression of SIRT1 in mice attenuates endoplasmic reticulum stress and insulin resistance in the liver.* Faseb j, 2011. **25**(5): p. 1664-79.

31. Xu, F., et al., *Lack of SIRT1 (Mammalian Sirtuin 1) activity leads to liver steatosis in the SIRT1+/- mice: a role of lipid mobilization and inflammation.* Endocrinology, 2010. **151**(6): p. 2504-14.

32. Mariani, S., et al., *Plasma levels of SIRT1 associate with non-alcoholic fatty liver disease in obese patients.* Endocrine, 2015. **49**(3): p. 711-6.

33. Wu, T., et al., *Direct evidence of sirtuin downregulation in the liver of non-alcoholic fatty liver disease patients.* Ann Clin Lab Sci, 2014. **44**(4): p. 410-8.

34. Chalasani, N., et al., *The diagnosis and management of non-alcoholic fatty liver disease: practice guideline by the American Gastroenterological Association, American Association for the Study of Liver Diseases, and American College of Gastroenterology.* Gastroenterology, 2012. **142**(7): p. 1592-609.

35. Loomba, R. and A.J. Sanyal, *The global NAFLD epidemic.* Nat Rev Gastroenterol Hepatol, 2013. **10**(11): p. 686-90.

36. Bugianesi, E., et al., *Insulin resistance in non-diabetic patients with non-alcoholic fatty liver disease: sites and mechanisms.* Diabetologia, 2005. **48**(4): p. 634-42.

37. Marchesini, G., et al., *Nonalcoholic fatty liver disease: a feature of the metabolic syndrome.* Diabetes, 2001. **50**(8): p. 1844-50.

38. Pathania, D., M. Millard, and N. Neamati, *Opportunities in discovery and delivery of anticancer drugs targeting mitochondria and cancer cell metabolism.* Adv Drug Deliv Rev, 2009. **61**(14): p. 1250-75.

39. Simões, I.C.M., et al., *Mitochondria in non-alcoholic fatty liver disease.* Int J Biochem Cell Biol, 2018. **95**: p. 93-99.

40. Rodrigues, P.M., et al., *miR-21 ablation and obeticholic acid ameliorate nonalcoholic steatohepatitis in mice.* Cell Death Dis, 2017. **8**(4): p. e2748.

41. Handa, P., et al., *Reduced adiponectin signaling due to weight gain results in nonalcoholic steatohepatitis through impaired mitochondrial biogenesis.* Hepatology, 2014. **60**(1): p. 133-45.

42. Koliaki, C., et al., *Adaptation of hepatic mitochondrial function in humans with non-alcoholic fatty liver is lost in steatohepatitis.* Cell Metab, 2015. **21**(5): p. 739-46.

43. Colak, Y., et al., *SIRT1 as a potential therapeutic target for treatment of nonalcoholic fatty liver disease.* Med Sci Monit, 2011. **17**(5): p. Hy5-9.

44. Ding, R.B., J. Bao, and C.X. Deng, *Emerging roles of SIRT1 in fatty liver diseases.* Int J Biol Sci, 2017. **13**(7): p. 852-867.

45. Faghihzadeh, F., et al., *Resveratrol supplementation improves inflammatory biomarkers in patients with nonalcoholic fatty liver disease.* Nutr Res, 2014. **34**(10): p. 837-43.

46. Chen, S., et al., *Resveratrol improves insulin resistance, glucose and lipid metabolism in patients with non-alcoholic fatty liver disease: a randomized controlled trial.* Dig Liver Dis, 2015. **47**(3): p. 226-32.

Figures
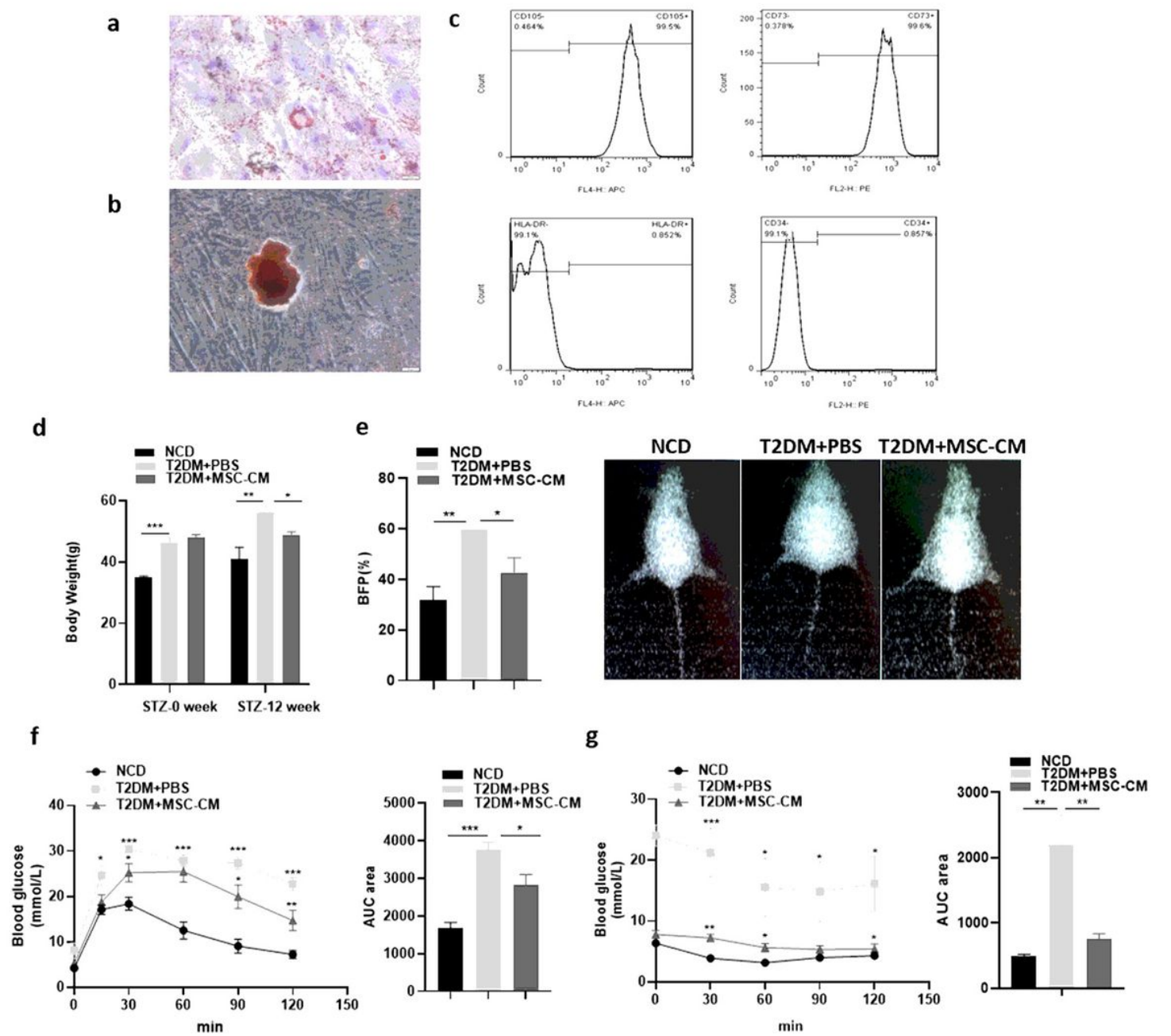
Figure 1

MSC-CM improves glucose tolerance in T2DM mice and increases insulin sensitivity. (a) Oil Red O staining of cultured adipogenic Hu-MSCs. (b) Alizarin Red staining of cultured osteogenic Hu-MSCs. (c) Flow cytometry analysis of Hu-MSCs surface markers (CD105 and CD73) and hematopoietic markers (HLA-DR and CD34). (d) Body weight of mice in the following groups: NCD, T2DM+PBS, and T2DM+MSC-CM. (e) The representative DEXA image shows the body fat percentage (BFP%) of the mice and the comparison of the three groups. (f) IPGTT results and corresponding areas under the curve and (g) IPITT results and corresponding areas under the curve were analyzed to assess insulin tolerance and insulin sensitivity at 2 weeks after the last infusion of PBS or MSC-CM. All results are expressed as the mean ± SEM (n = 8 mice per group; *P < 0.05; **P < 0.01; ***P < 0.001).
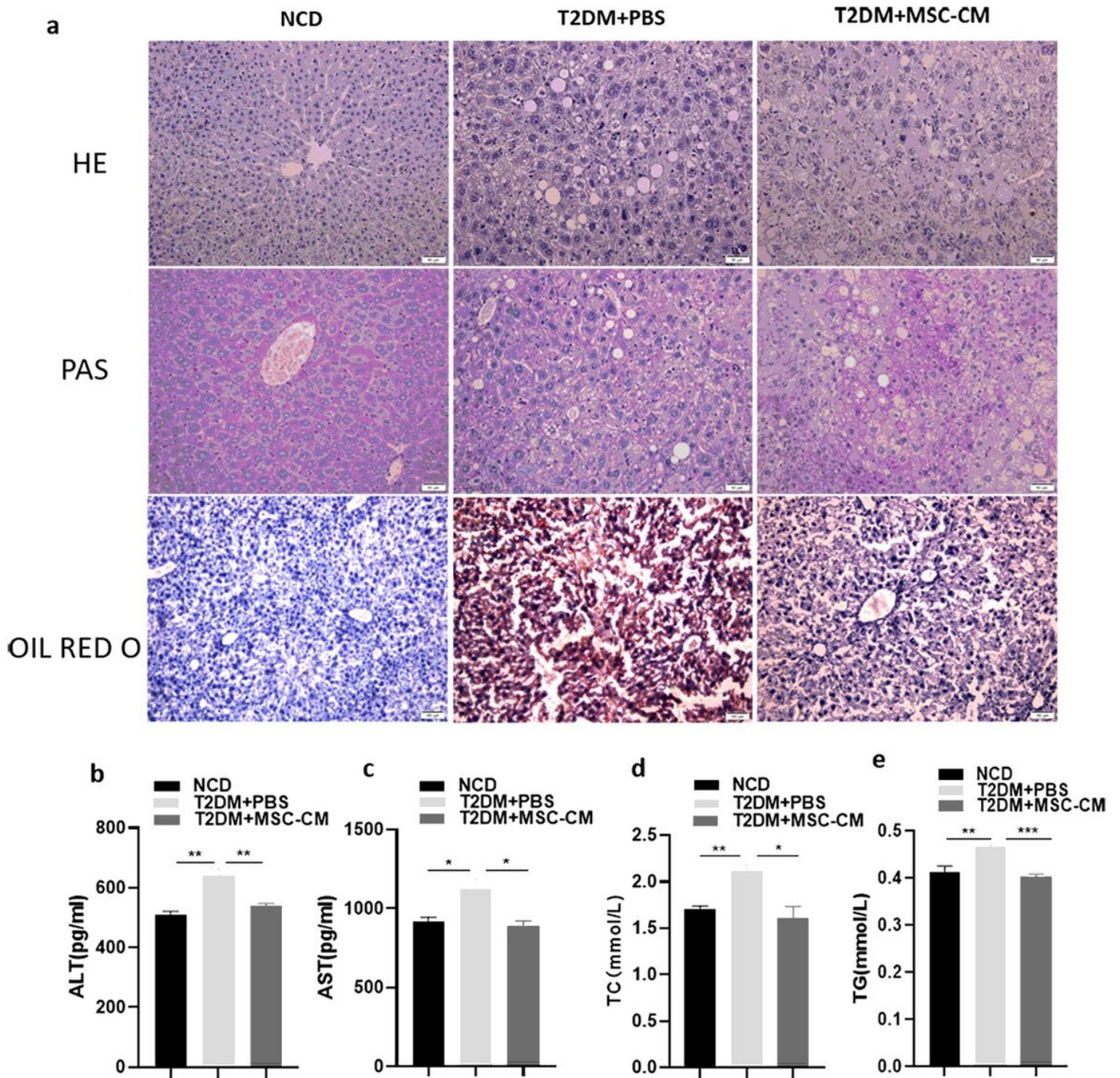
Figure 2

MSC-CM ameliorated the pathological changes in the livers of T2DM mice and serum metabolism indexes. (a) HE staining, PAS staining, and Oil Red O staining of three groups. Serum was collected to measure the levels of (b) ALT, (c) AST, (d) TC, and (e) TG. Data are expressed as the mean ± SEM (n = 5; *P < 0.05; **P < 0.01; ***P < 0.001).
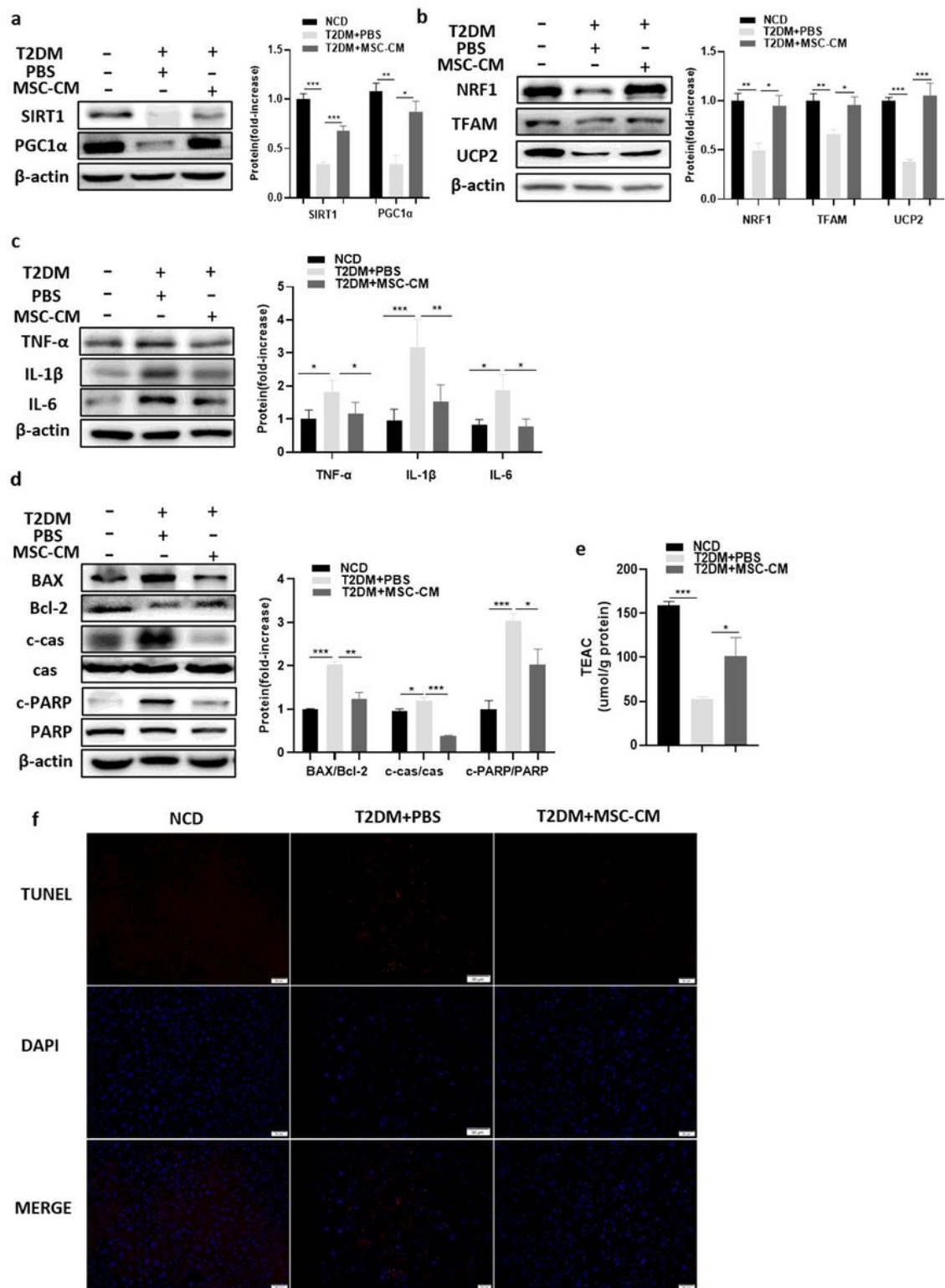
Figure 3

MSC-CM improves mitochondrial function, inflammation, and apoptosis in liver in vivo. (a) Protein levels of SIRT1 and PGC1α in the liver were analyzed by western blot in the NCD, T2DM+PBS, and T2DM+MSC-CM groups. (b) Protein levels of the key mitochondrial transcription factors NRF1, TFAM, and UCP2 in liver were analyzed by western blot. (c) Inflammation was assessed by measuring TNF-α, IL-1β, and IL-6 levels in the liver. (d) Apoptosis was assessed by calculating the BAX/Bcl-2, cleaved caspase 3/caspase

3, and cleaved PARP/PARP ratios and by TUNEL staining (f). (e) Trolox equivalent antioxidant capacity (TEAC) of three groups. Data are expressed as the mean ± SEM (n = 3; *P < 0.05; **P < 0.01; ***P < 0.001).
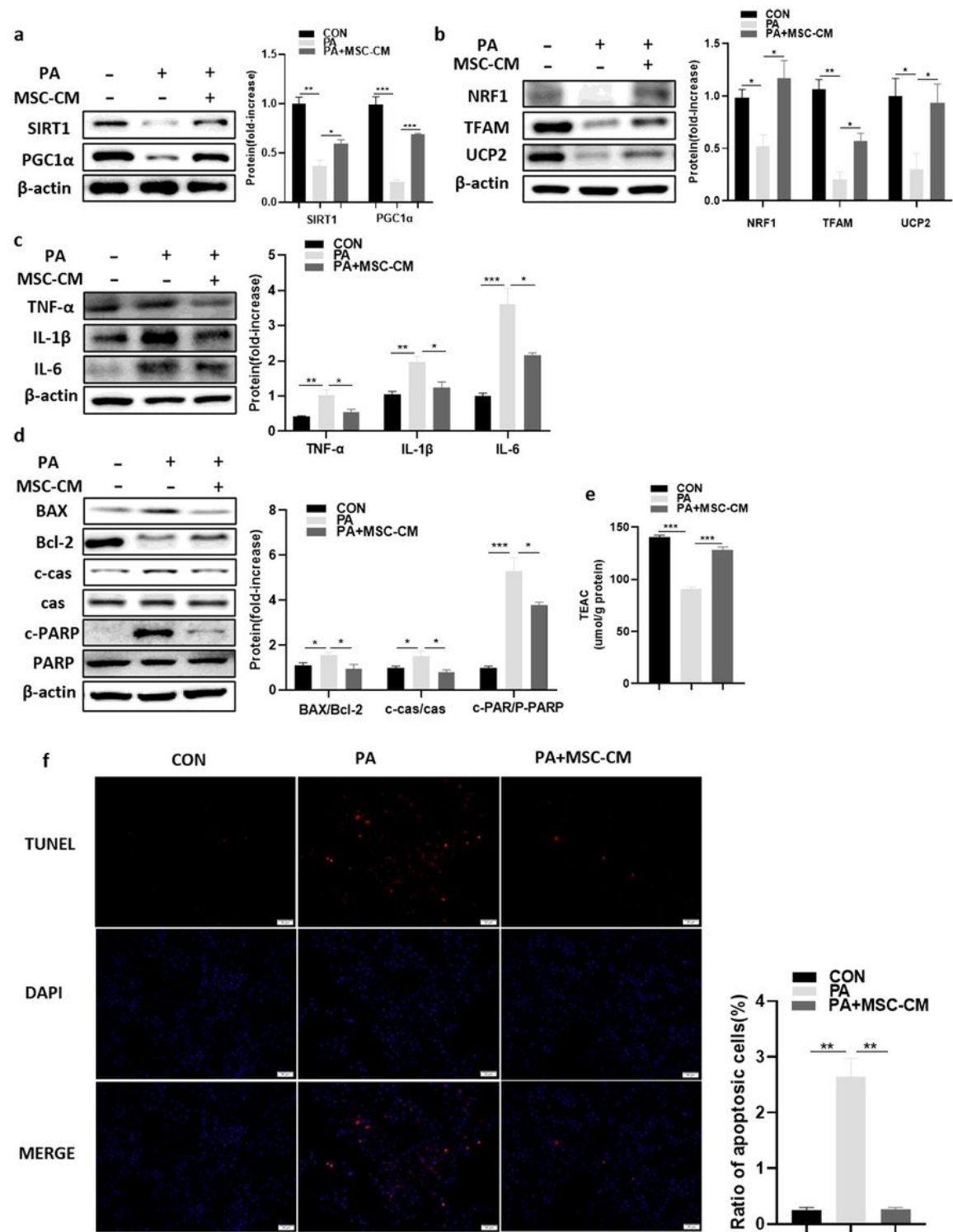

Figure 4

MSC-CM improves mitochondrial function and reduces inflammation and apoptosis of PA-stimulated L-O2 cells in vitro. (a) Protein levels of SIRT1 and PGC1α in L-O2 cells were analyzed by western blot in the CON, PA, and PA+MSC-CM groups. (b) Protein levels of NRF1, TFAM, and UCP2 in L-O2 cells were

analyzed by western blot. (c) Inflammation was assessed by measuring TNF-α, IL-1β, and IL-6 levels in the liver. (d) Apoptosis was assessed by calculating the BAX/Bcl-2, cleaved caspase 3/caspase 3, and cleaved PARP/PARP ratios in L-O2 cells and by TUNEL staining (f). (e) Trolox equivalent antioxidant capacity (TEAC) of three groups. Data are expressed as the mean ± SEM (n = 3; *P < 0.05; **P < 0.01; ***P < 0.001).
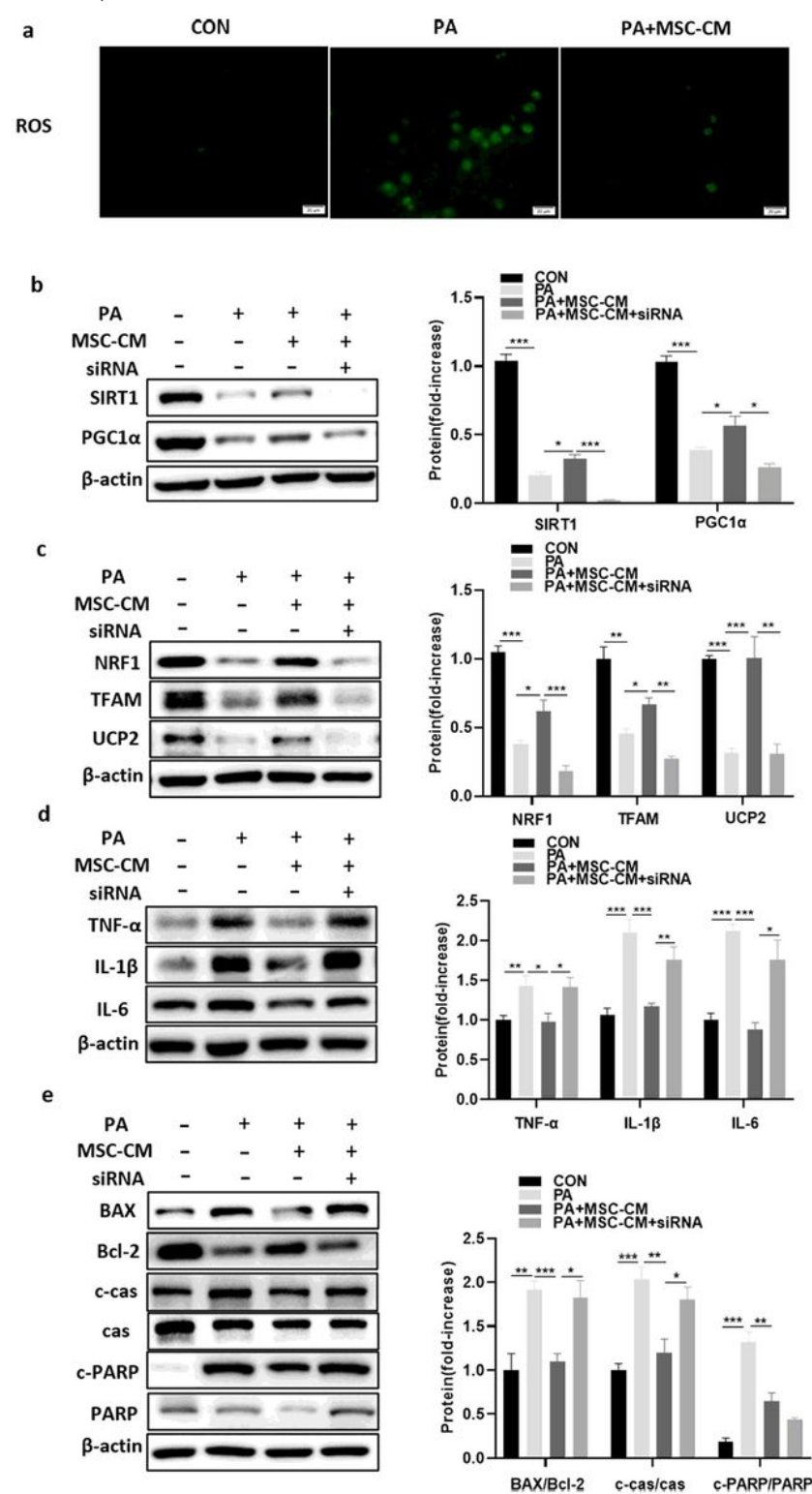

Figure 5

The positive effects of MSC-CM were offset when SIRT1 was silenced. (a) Representative fluorescence images of ROS show production of ROS in L-O2 cells. (b) Protein levels of SIRT1 and PGC1α in L-O2 cells of the CON, PA, PA+MSC-CM, and PA+MSC-CM+ siRNA groups. (c) Protein levels of NRF1, TFAM, and UCP2 in L-O2 cells were analyzed by western blot. (d) Inflammation was estimated by measuring TNF-α, IL-1β, and IL-6 levels. (e) Apoptosis was estimated by calculating the BAX/Bcl-2, cleaved caspase 3/caspase 3, and cleaved PARP/PARP ratios. Data are expressed as the mean ± SEM (n = 3; *P < 0.05; **P < 0.01; ***P < 0.001).
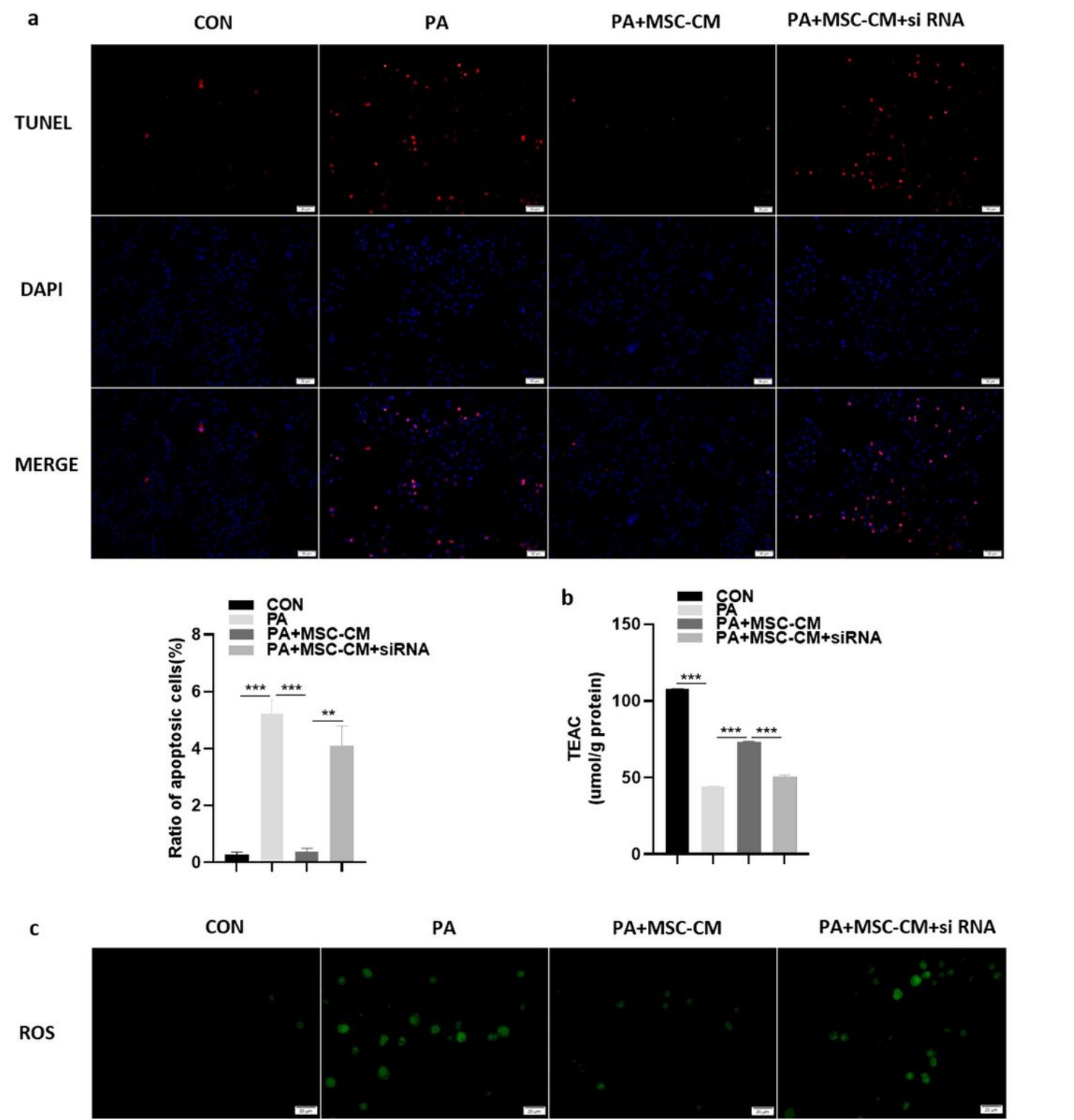
Figure 6

The positive effects of MSC-CM were offset when SIRT1 was silenced. (a) Apoptosis was estimated by TUNEL staining. (b) Trolox equivalent antioxidant capacity (TEAC) of four groups. (c) Representative fluorescence images of ROS show production of ROS in L-O2 cells of four groups. Data are expressed as the mean ± SEM (n = 3; *P < 0.05; **P < 0.01; ***P < 0.001).